Hindawi Publishing Corporation
Modelling and Simulation in Engineering
Volume 2014, Article ID 524824, 9 pages
http://dx.doi.org/10.1155/2014/524824

Research Article

Interaction of Submerged Breakwater by a Solitary Wave Using WC-SPH Method

Afshin Mansouri[1] and Babak Aminnejad[2]

[1] *Departmentof Civil Engineering, The Islamic Azad University of Roudehen Branch, Tehran, Iran*
[2] *Department of Civil Engineering, Faculty of Civil Engineering, The Islamic Azad University of Roudehen Branch, Tehran, Iran*

Correspondence should be addressed to Afshin Mansouri; afshinmansoori@gmail.com

Received 3 January 2014; Revised 8 March 2014; Accepted 11 March 2014; Published 13 April 2014

Academic Editor: Agostino Bruzzone

Interaction of a solitary wave and submerged breakwater is studied in a meshless, Lagrangian approach. For this purpose, a two-dimensional smoothed particle hydrodynamics (SPH) code is developed. Furthermore, an extensive set of simulations is conducted. In the first step, the generated solitary wave is validated. Subsequently, the interaction of solitary wave and submerged breakwater is investigated thoroughly. Results of the interaction of solitary wave and a submerged breakwater are also shown to be in good agreement with published experimental studies. Afterwards, the effects of the inclination and length of breakwater as well as distance between two breakwaters are evaluated on damping ratio of breakwater.

1. Introduction

Due to development of ports and marine, protection of the seashores against the sea waves must be considered as an important issue in the field of marine structure. In this context, breakwaters have been used as appropriate tools in previous decades. A wide range of breakwaters has been introduced, so far. Submerged breakwater is one of them which has been utilized in many countries. Generally, some advantages of submerged breakwater can be mentioned as follows:

(1) simple structure,

(2) cost effectiveness,

(3) safety of marine transport vessels,

(4) short construction period,

(5) preserving beauty of the coast (touristy aspect),

(6) high strength of the structures against sea waves,

(7) preventing coastal erosion area with scattering of wave energy.

In addition, the performance of submerged breakwaters depends on geometry, material properties, and environmental characteristics of surrounding breakwater [1]. In the following paragraphs, several studies dealing with the submerged breakwaters are reviewed.

Effects of overtopping submerged obstacle on wave characteristics were investigated by Hara et al. [2]. They used a numerical model as well as a regression method to calculate the rate of the wave breaking. Hayakawa et al. [3] also studied flow field around a trapezoidal submerged breakwater numerically. They compared the obtained 2D and 3D numerical results with an experimental finding. Solitary wave interaction with submerged multibodies was considered by Wan Decheng and Guoxiong [4] theoretically. An experimental investigation of the wave transmission on submerged breakwaters was also considered by Armono and Hall [5]. An experimental comparison of wave field behind a submerged trapezoidal breakwater and double submerged trapezoidal breakwater was performed by Yoshida et al. [6]. In their study, the ratio between breakwaters and the wave height has been studied. Interaction of a solitary wave and permeable rectangular submerged breakwater had been evaluated by Huang et al. [7]. They measured the wave

transmission as well as the amount of dragon the breakwater. Stamos et al. [8] performed an experimental study and considered performance of absorption and reflection of waves from hemicylindrical and rectangular submerged breakwaters. Johnson et al. [9] conducted an experimental and theoretical study of currents and waves around trapezoidal submerged breakwater. Muni-Reddy and Neelamani [10] presented a numerical and experimental investigation for measurement of wave breaking and force on a protected offshore base with trapezoidal breakwater. Chen et al. [11] experimentally studied transformation of waves with various profiles, between a trapezoidal submerged breakwater and sea wall. Christou et al. [12] presented numerical simulation of regular nonlinear waves interaction with rectangular submerged breakwaters for investigation of transmitted and reflected waves profile. Zaman et al. [13] investigated the amount of deformation of waves passing over the parabolic breakwater and the extent of waves reflected area. Losada et al. [14] investigated transmission, reflection, turbulence, and breakage of regular and irregular waves overtopping of rubble mound breakwaters. Cao et al. [15] numerically studied hydrodynamic properties of wave propagation which surrounded two impermeable trapezoidal submerged breakwaters.

In the area of breakwater computations, smoothed particle hydrodynamics (SPH) can also be implemented as a novel meshless numerical method that is being developed for the study of near shore waves and navy needs. In this context, several numerical models have been developed with SPH method for modeling free surface flows. Dalrymple et al. [16], Gotoh et al. [17], and Shao [18] have presented some numerical techniques in conjunction with SPH which have been widely used. Furthermore, Dalrymple and Rogers [19] showed that SPH method offers a variety of advantages for fluid modeling, especially those with a free surface. Yim et al. [20] investigated wave's interaction with porous rigid semisubmerged rectangular breakwater with RANS and SPH methods. Cherfils et al. [21] also considered flow surrounding a horizontal submerged plate as a breakwater near shores with SPH method. Didier and Neves [22] studied wave speed, wave height, and breakage of wave over sloped sea wall for a region of the Portuguese with SPH method.

Furthermore, to simulate water waves with SPH, many different approaches have been presented, so far. Shao [23] offered a coupled incompressible smoothed particle hydrodynamics (ISPH) porous medium method to simulate free surface profile. Liu et al. [24] optimized 3D SPH method for application of water wave modeling. Generally, interested reader can refer to some articles [25, 26] for finding review literature of SPH development.

Due to necessity of obtaining appropriate comparison between the different factors affecting the performance of submerged breakwater and lack of widespread study on submerged breakwaters with SPH method, a relatively extensive parametric study on trapezoidal submerged breakwaters is presented. For this purpose, various geometrical aspects of breakwater are considered and a comparative study is performed. Furthermore, it is being tried to introduce an appropriate combination of numerical techniques in SPH for accurate simulation of solitary wave-breakwaters interaction.

2. Governing Equations

In smooth particle hydrodynamics, fluid flow can be represented by N discrete particles. Each of these particles may be specified by an individual mass. Moreover, particles move according to the equations of Newtonian mechanics, including a pressure force. For each of these particles, the equations are based on Lagrangian form of the Navier-Stokes equations:

$$\begin{aligned} \frac{d\rho}{dt} &= -\rho \nabla . v, \\ \frac{dv}{dt} &= -\frac{1}{\rho}\nabla p + g + \Pi, \end{aligned} \tag{1}$$

where v, p, and ρ are the velocity, pressure, and density, respectively. g is the gravitational acceleration and Π refers to the diffusion terms.

3. SPH Formulation

Navier-Stokes equations solution in SPH method is by defining a kernel function $W(x - x', h)$ around every x' location of an SPH particle. The maximum of this function occurs at $x = x'$. The features of kernel function must be similar to Dirac Delta function. Therefore, behavior of kernel function is completely dependent on value of $r = x - x'$. The value h is the parameter which defines the "size" of influence area of kernel function and is called the smoothing length. The kernel is normalized to unity in the following way:

$$\int_{\Omega} W\left(x - x', h\right) dx' = 1, \tag{2}$$

and we also have

$$\lim_{h \to 0} W\left(x - x', h\right) = \delta\left(x - x'\right). \tag{3}$$

We should regard the SPH kernel as a defining region of influence of the SPH particle. It will turn out with only SPH particles which lie within each other's regions of influence and are able to interact with each other.

Furthermore, kernel function is implemented to approximate field variables at any point in a computational domain. For instance, an estimate value of a function $f(x)$ at the location x is given in a continuous form by an integral of the product of the function and a kernel function $W(x - x', h)$:

$$\langle f(x) \rangle = \int_{\Omega} f\left(x'\right) W\left(x - x', h\right) dx', \tag{4}$$

where the angle brackets $\langle\rangle$ denote a kernel approximation. In addition to the abovementioned characteristics, kernel function must satisfy several other features such as positivity condition [27]. Moreover, (4) can be also approximated by a summation as follows:

$$\langle f(x) \rangle \cong \sum_{j} \frac{m_j}{\rho_j} f\left(x_j\right) W\left(\left|x - x'\right|, h\right), \tag{5}$$

where m_j/ρ_j is the volume associated with the particle j. This equation can be used if the function $f(x)$ is only known at N discrete points.

The kernel function description can be finalized by defining a specific kernel function. Numerous possibilities exist. A large number of kernel function types are discussed in literature, ranging from polynomial to Gaussian. The most common is the B-spline kernel that was proposed by Monaghan and Lattanzio [28]:

$$w(r,h) = \alpha_D \begin{cases} 1 - \frac{3}{2}q^2 + \frac{3}{4}q^3 & 0 \le q \le 1 \\ \frac{1}{4}(2-q)^3 & 1 \le q \le 2 \\ 0 & q \ge 2 \end{cases} \tag{6}$$

which is considered in the present paper and $q = r/h$ and α_D is equal to $10/\pi h^2$ in two dimensional cases.

4. SPH Implementation on Governing Equations

Now, based on the SPH formulation, mentioned in previous section, governing equations will be discretized. In this context, the continuity equation for particle i can be considered in the SPH formulation as

$$\frac{d\rho_i}{dt} = -\sum_{j=1}^{N} m_j \left(v_j - v_j\right) \cdot \nabla W_{ij}, \tag{7}$$

where the sum extends over all neighboring particles and W is the smoothing kernel evaluated at the distance between particles i and j.

The SPH formulation of the momentum equations based on artificial viscosity can also be obtained through the particle approximation procedure as in

$$\frac{dv_i}{dt} = -\sum_{j=1}^{N} m_j \left(\frac{P_i}{\rho_i^2} + \frac{P_j}{P_j^2} + \Pi_{ij}\right) \nabla W_{ij} + g, \tag{8}$$

where Π_{ij} is the viscosity term. To introduce viscous dissipation, an artificial viscosity concept which has been developed using Monaghan [29] is implemented. This term is symmetric, conserves momentum, and introduces a shear viscosity into the momentum equation. The SPH form of the momentum equation is written as

$$\Pi_{ab} = \begin{cases} \dfrac{-\alpha \overline{C_{ab}} \mu_{ab}}{\overline{\rho_{ab}}} V_{ab} \cdot r_{ab} < 0, \\ 0, \text{ for other values,} \end{cases} \tag{9}$$

where

$$\mu_{ab} = \frac{h v_{ab} \cdot r_{ab}}{r_{ab}^2 + \eta^2}, \tag{10}$$

$$\overline{\rho}_{ab} = \frac{1}{2}\left(\rho_a + \rho_b\right), \qquad \overline{C}_{ab} = \frac{1}{2}\left(C_a + C_b\right); \qquad \eta^2 = 0.01h^2. \tag{11}$$

α is also a constant. Monaghan [29] suggests that a value of $\alpha = 0.01$ can be used for most computations.

5. Numerical Details

5.1. XSPH Technique. To modify the particle's velocity, XSPH technique is used and particle i is moved based on this technique. In XSPH scheme, it is formulated as follows:

$$\frac{dr_i}{dt} = v_i + \varepsilon \sum_j \frac{m_j}{\overline{\rho}_{ij}} v_{ij} W_{ij}. \tag{12}$$

Velocity of particle i is recalculated in such manner that the velocity of particle i and the average velocity of the closest neighborhood particles interacting with particle i are taken into account.

5.2. Time Stepping Procedure. In the present paper, predictor-corrector time stepping algorithm is implemented. In the predictor-corrector formulation, variation of particles properties (such as velocity) is estimated as [17]. Consider

$$v_i^{n+1/2} = v_i^n + \frac{\Delta t}{2} F_i^{n+1/2}. \tag{13}$$

And by implementing forces at half step, the values of velocity can be calculated at the end of any step which is formulated as follows [17]:

$$v_i^{n+1} = 2v_i^{n+1/2} - v_i^n. \tag{14}$$

5.3. Density Filter. In weakly compressible SPH formulation, large pressure oscillation has been observed. These pressure inaccuracies can be modified using some procedures. In addition to pressure modification, the free surface profile will be also improved. Therefore, MLS (moving least square) density filter which is a first order density correction is used to reproduce the linear variation of the density field:

$$\overline{\rho}_a = \sum_b \rho_b W_{ab}^{\text{MLS}} \frac{m_b}{\rho_b} = \sum_b m_b W_{ab}^{\text{MLS}}. \tag{15}$$

The corrected kernel is also evaluated as follows:

$$W_{ab}^{\text{MLS}} = W_{ab}^{\text{MLS}}\left(r_a\right) = \beta\left(r_a\right) \cdot \left(r_a - r_b\right) W_{ab}. \tag{16}$$

More details can be found in many references in the literature [30, 31].

5.4. Boundary Conditions. Two rows of stationary water particles at the boundary (Figure 1) remain fixed or move according to an externally imposed function for, say, wave maker boundaries. When a fluid particle approaches the boundary, the density and hence pressure exerted by the boundary particles increase. This generates the necessary repulsive force on the water particles. A major deficiency of this method is the generation of numerical boundary layers. When water particles get close to the boundary particles, they tend to stick to the boundary; thus they generate a boundary layer which is not physically observed.

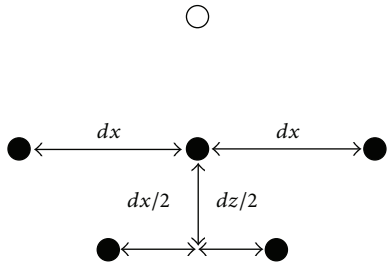

Figure 1: Interaction between fluid particles and boundary particles.

6. Solitary Wave Generation

Solitary wave is generated by Prescribe Piston Wave Maker [5]. Value of paddle displacement is applied in the following equation [22]:

$$X_p(t) = \frac{H}{k}\left[\tanh(X(t)) + \tanh\left(\frac{k}{d}\lambda\right)\right];$$
$$X(t) = \frac{k}{d}\left(ct - X_p(t) - \lambda\right), \tag{17}$$

where H is the wave height, $k = \sqrt{((3H/4d))}$ is wave number, and $c = \sqrt{(g(d + H))}$ is speed. Wave speed can also be obtained from the following equation [22]:

$$u_p(t) = \frac{cH}{d}\frac{1}{\cosh^2 X(t) + (H/d)}. \tag{18}$$

6.1. Validation of Generated Solitary Wave. According to Maiti and Sen [32] simulation which is a benchmark test, the length and flat length of the tank, water depth, and slope of the right hand side of the tank were, respectively, considered to be 10 m, 9.7 m, 0.3 m, and 45 degree (Figure 2). The motion of wave paddle is calculated for $H/d = 0.1$. Therefore, wave height and λ are 0.03 and 6.882.

The result of solitary wave generation is illustrated in Figure 3. Simulation is conducted from 0 till 10 sec. It is observed that the wave height is equal to 0.03 m and obtained free surface profile is relatively accurate for further studies. However, some inconsistencies are visible at second 4. In addition, average error of SPH simulation (point to point) is equal to 1.89 percent.

7. Results and Discussion

In this section, various aspects of solitary wave-breakwater interaction will be studied. At first step, free surface related to a specific breakwater under interaction with a solitary wave is computed using SPH to ensure that our numerical setup is suitable for investigation of more complicated problems. Afterward, various geometrical characteristics of breakwaters are also discussed. For more detailed studies, two breakwaters are considered and effects of distance between these breakwaters will be evaluated.

7.1. Validation. For further evaluation of SPH accuracy, the free surface profile, generated in solitary wave-breakwater interaction, is compared with experimental work of Grilli et al. [33]. To perform this comparison, a computational domain is defined (Table 1). Furthermore, the characteristics of wave flume, solitary wave, and breakwater are presented. Results of this simulation are illustrated at Figure 4. Features of the presented simulation are also reported in Table 2. Free surface profiles in Figure 4(a) through 4(d) are at 10, 11.81, 13, and 13.92 sec, respectively. RMS of obtained solutions which are calculated relative to experimental findings seem to be reasonable. Therefore, it can be declared that our numerical setup can model solitary wave-breakwater interaction with satisfying precision.

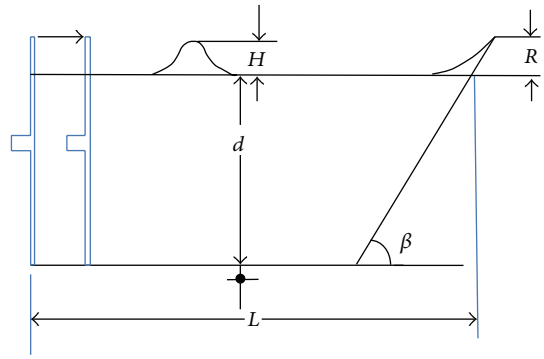

Figure 2: Computational domain.

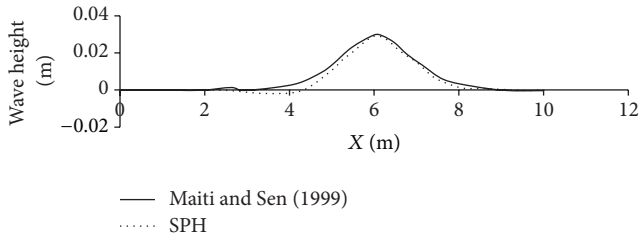

Figure 3: Comparison of generated solitary wave with Sagnita's results.

Table 1: Wave flume, solitary wave, and breakwater features.

Value	Characteristics
0.3 m	Wave height (H)
1.0 m	Water depth (d)
45 m	(L_0)
70 m	(L_{overal})
0.8 m	Height of breakwater (h)
0.4 m	Breakwater's beam
1 : 2	Slope of breakwater's wall

7.2. Investigation of Breakwater Inclination. A subject studied here is considering the effects of breakwater's slope on H/H' ratio. For this purpose, computational domain as well as solitary wave is considered to be the same as previous section. Slope of breakwater, at aft part (β_2), which is shown in Figure 5 is varied systematically. All considered angles are

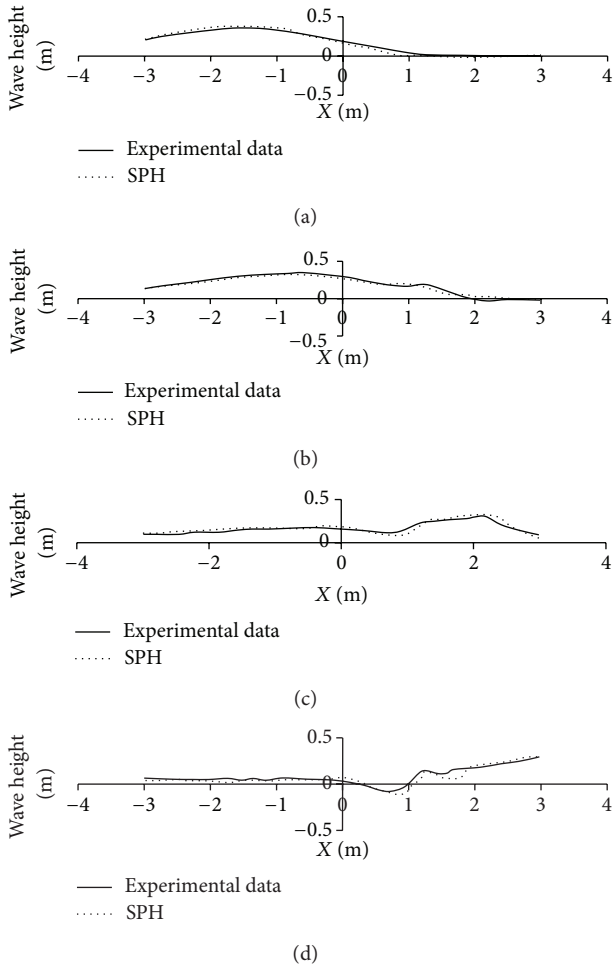

Figure 4: Comparison of SPH's free surface profile with experimental data [33].

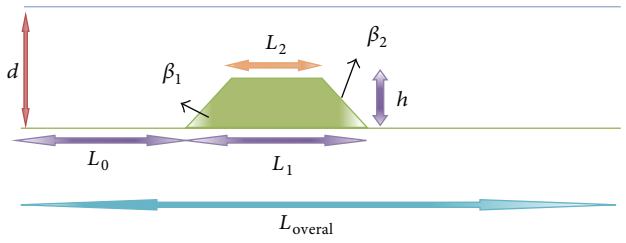

Figure 5: Computational domain.

Table 2: Computational error.

Time (sec)	Figure	RMS
10	Figure 4(a)	0.036
11.81	Figure 4(b)	0.034
13	Figure 4(c)	0.049
13.92	Figure 4(d)	0.053

presented in Table 3. Furthermore, geometrical characteristics of breakwater are also proposed in this table.

Table 3: Breakwater's characteristics.

β_2	β_1	h	L_1
0	$\tan^{-1}(0.5)$	0.4	2
15	$\tan^{-1}(0.5)$	0.4	2
45	$\tan^{-1}(0.5)$	0.4	2
60	$\tan^{-1}(0.5)$	0.4	2
75	$\tan^{-1}(0.5)$	0.4	2
90	$\tan^{-1}(0.5)$	0.4	2

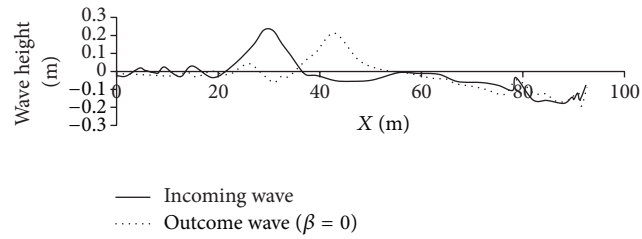

Figure 6: Free surface profile for $\beta_2 = 0$ degree.

Free surface profile related to each considered condition is illustrated in Figures 6, 7, 8, 9, 10, and 11. In each case, obtained free surface profile is compared with generated solitary wave without considering breakwater effect. Exact evaluation of breakwater's slope on the free surface profile is presented in Table 4. It is obvious that wherever $\beta_2 = 90$, maximum wave reduction can be achieved. Correspondingly, when β_2 decreased to zero, minimum breakwater effect occurs. Generally, Figure 12 also shows a representative frame of SPH solution.

7.3. Investigation of Breakwater Length. To perform further parametric studies, the effects of breakwater's length on free surface can also be evaluated. In this context, previous computational characteristics are kept and only the length ratio L_1/L_2 is changed systematically. Considered situations are presented in Table 5. Figures 13 and 16 show the obtained results at various length ratios. In all cases, breakwater generates a hollow in free surface at breakwater position which leads to a reduction in wave crest. Generally, based on Table 6, it is observed that L_1/L_2 ratio decreased, so breakwater performance will be improved. In addition, it can be concluded that smaller length ratio leads to more reduction of wave amplitude. To complete this section, a view of SPH solution is also presented in Figure 17.

7.4. Investigation of Distance between Two Submerged Breakwaters. In this part, influences of distance variation between two breakwaters are evaluated. Distance between two breakwaters (X) is considered to be less than wavelength at the beginning of simulations. Consequently, this distance will increase until the gap becomes larger than the wavelength. In addition, wave height, water depth, and length of wave flume are considered to be $H = 0.3$ m, 1.2 m, and 70 m, successively. Breakwater is located 30 meters from the left. Geometrical characteristics of breakwaters are also presented

Table 4: Effect of breakwater slope on H/H' ratio.

Values	$\beta_2 = 0$	$\beta_2 = 15$	$\beta_2 = 45$	$\beta_2 = 60$	$\beta_2 = 75$	$\beta_2 = 90$
H/H'	1.078973	1.185936	1.297549	1.32081	1.470258	1.503094

Table 5: Geometrical characteristics.

L_1/L_2	β_1	β_2	L_2	L_1
9	$\tan^{-1}(0.5)$	$\tan^{-1}(0.5)$	0.2	1.8
6.33	$\tan^{-1}(0.5)$	$\tan^{-1}(0.5)$	0.3	1.9
4.2	$\tan^{-1}(0.5)$	$\tan^{-1}(0.5)$	0.5	2.1
3.67	$\tan^{-1}(0.5)$	$\tan^{-1}(0.5)$	0.6	2.2

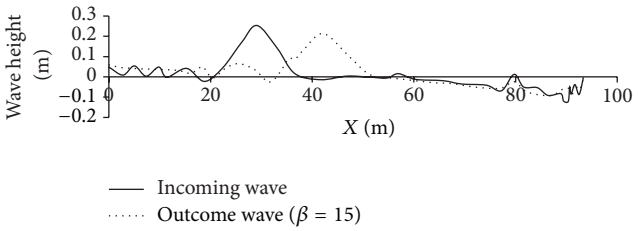

Figure 7: Free surface profile for $\beta_2 = 15$ degree.

in Table 7. Figure 18 shows the gap effects between two considered breakwaters. It is observed that when wave reaches the first breakwater, the wave height is equal to 0.25 m. However, second breakwater decreases the wave height in correspondence with considered distance between two breakwaters. In this context, two parameters, H (wave height above first breakwater) and H' (wave height above second breakwater), are introduced. Breakwater influence coefficient is also defined as H/H'. Precise values of defined parameter are presented in Table 8. It is obviously clear that, for $X = 0.3$ m, maximum wave reduction is achieved. Furthermore, it can be concluded that optimum gap between breakwaters is affected by wave length. In reality, when gap between breakwaters is smaller than wave length, effects of second breakwater will be decreased. Additionally, maximum effectiveness of breakwater is observed whenever the distance is equal to wave length. A representation of our SPH solution is also depicted in Figure 19.

8. Results

The present paper focuses on the breakwater performance under a solitary wave. Furthermore, we have tried to implement meshless and Lagrangian approach of smoothed particle hydrodynamics method to study considered physics. In this context, a two-dimensional SPH code is developed. To consider diffusion terms, an artificial viscosity model is included. Particles movement is also calculated using XSPH variant and predictor-corrector scheme which is investigated as time stepping algorithm. To reinitialize density field, MLS density filter is utilized.

To start computations, generated solitary wave is verified by comparing previous studies. Afterwards, a breakwater

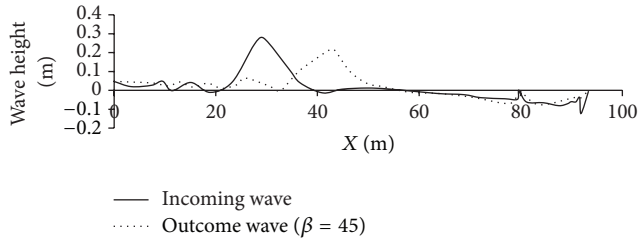

Figure 8: Free surface profile for $\beta_2 = 45$ degree.

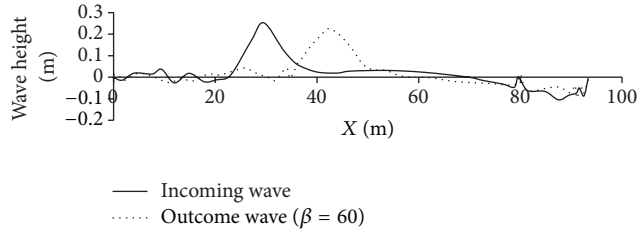

Figure 9: Free surface profile for $\beta_2 = 60$ degree.

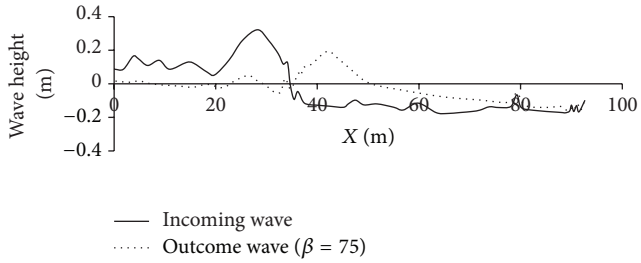

Figure 10: Free surface profile for $\beta_2 = 75$ degree.

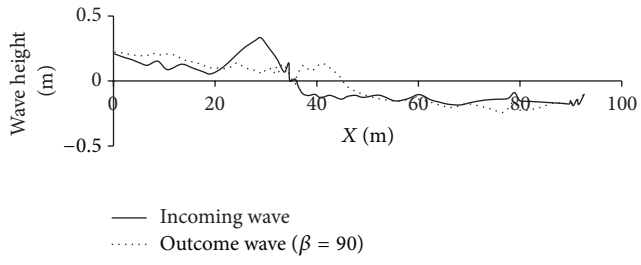

Figure 11: Free surface profile for $\beta_2 = 90$ degree.

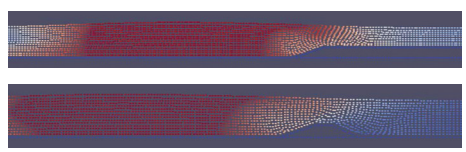

Figure 12: A representative frame of SPH solution.

Table 6: Exact evaluation of length ratio effect on free surface reduction.

Values	$L_1/L_2 = 9$	$L_1/L_2 = 6.33$	$L_1/L_2 = 4.2$	$L_1/L_2 = 3.67$
H/H'	1.094116	1.105263	1.111112	1.222223

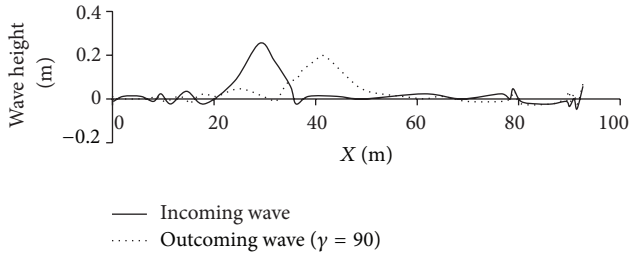

Figure 13: Free surface profile with ratio 9 in length.

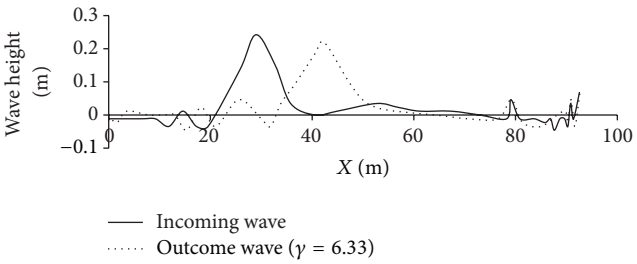

Figure 14: Free surface profile at length ratio 6.33.

Table 7: Breakwater characteristics.

(X)	Left side slope	Right side slope	Breakwater height	Lower length
0.2	$\tan^{-1}(0.5)$	$\tan^{-1}(0.5)$	0.4	2
0.3	$\tan^{-1}(0.5)$	$\tan^{-1}(0.5)$	0.4	2
0.4	$\tan^{-1}(0.5)$	$\tan^{-1}(0.5)$	0.4	2
0.5	$\tan^{-1}(0.5)$	$\tan^{-1}(0.5)$	0.4	2

Table 8: Effects of breakwaters distance.

Damping ratio	$X = 0.2$	$X = 0.3$	$X = 0.4$	$X = 0.5$
H/H'	1.247285	1.42718	1.3381	1.337985

is also included in computational domain. To validate our SPH solutions, obtained free surface profile is compared with existing experimental results and it is observed that our SPH solutions have a reasonable accuracy. In the second phase, various geometrical aspects of breakwater are also studied.

Generally, effects of implementing two breakwaters, inclination of breakwater, and breakwater's length on free surface depression are evaluated. It is found that when gap between breakwaters is smaller than wave length, effects of second breakwater will be decreased. Maximum effectiveness of breakwater also occurred whenever the distance is equal to wave length. In addition, when the inclination of breakwater increased, free surface deformation will be modified. Furthermore, it is observed that length ratio of breakwater can effectively influence free surface profile (Figures 14 and 15).

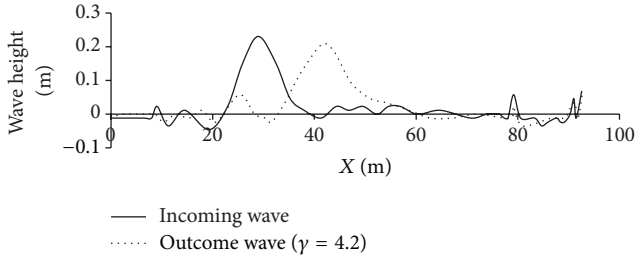

Figure 15: Free surface profile at length ratio 4.2.

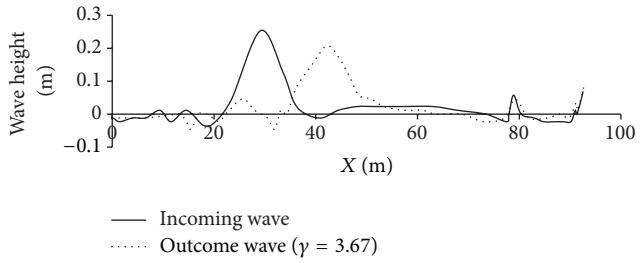

Figure 16: Free surface profile at length ratio 3.67.

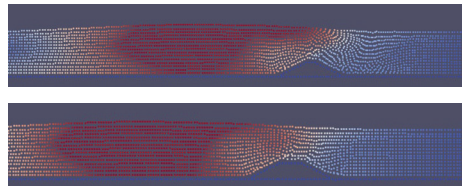

Figure 17: A view of SPH solution.

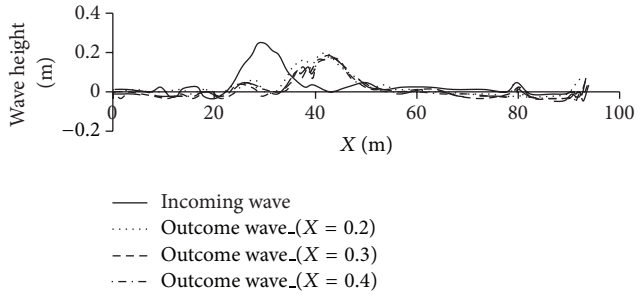

Figure 18: Simulated free surface profiles at different distances between breakwaters.

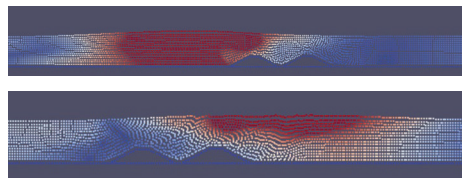

Figure 19: Particle representation of SPH solution.

To perform more precise computation, extending SPH solutions to three-dimensional case will be in attendance. Various simple breakwater geometries will also be introduced in near future.

Conflict of Interests

The authors declare that there is no conflict of interests regarding the publication of this paper.

References

[1] S. Tokura and T. Ida, "Simulation of wave dissipation mechanism on submerged structure using fluid-structure coupling capability in LS-DYNA," in *Proceedings of the 5th European LS-DYNA Conference*, 2005.

[2] M. Hara, T. Yasuda, and Y. Sakakibara, "Characteristics of a solitary wave breaking caused by a submerged obstacle," *Coastal Engineering*, vol. 1, no. 23, 1992.

[3] N. Hayakawa, T. Hosoyamada, S. Yoshida, and G. Tsujimoto, "Numerical simulation of wave fields around the submerged breakwater with SOLA-SURF method," in *Proceedings of the 26th International Conference on Coastal Engineering (ICCE '98)*, pp. 843–852, June 1998.

[4] W. Decheng and W. Guoxiong, "Numerical simulation of a solitary wave interaction with submerged multi-bodies," *Acta Mechanica Sinica*, vol. 14, no. 4, pp. 304–305, 1998.

[5] H. D. Armono and K. R. Hall, "Wave transmission on submerged breakwaters made of hollow hemispherical shape artificial reefs," in *Canadian Coastal Conference*, pp. 313–322, June 2003.

[6] A. Yoshida, S. Yan, M. Yamashiro, and I. Irie, "Wave Field Behind a Double-Submerged Breakwater," in *Proceedings of the 12th International Offshore and Polar Engineering Conference*, pp. 785–790, May 2002.

[7] C.-J. Huang, H.-H. Chang, and H.-H. Hwung, "Structural permeability effects on the interaction of a solitary wave and a submerged breakwater," *Coastal Engineering*, vol. 49, no. 1-2, pp. 1–24, 2003.

[8] D. G. Stamos, M. R. Hajj, and D. P. Telionis, "Performance of hemi-cylindrical and rectangular submerged breakwaters," *Ocean Engineering*, vol. 30, no. 6, pp. 813–828, 2003.

[9] H. K. Johnson, T. V. Karambas, I. Avgeris, B. Zanuttigh, D. Gonzalez-Marco, and I. Caceres, "Modelling of waves and currents around submerged breakwaters," *Coastal Engineering*, vol. 52, no. 10-11, pp. 949–969, 2005.

[10] M. G. Muni-Reddy and S. Neelamani, "Wave interaction with caisson defenced by an offshore low-crested breakwater," *Journal of Coastal Research*, no. 39, pp. 1767–1770, 2006.

[11] H.-B. Chen, C.-P. Tsai, and C.-C. Jeng, "Wave transformation between submerged breakwater and seawall," *Journal of Coastal Research*, no. 50, pp. 1069–1074, 2007.

[12] M. Christou, C. Swan, and O. T. Gudmestad, "The interaction of surface water waves with submerged breakwaters," *Coastal Engineering*, vol. 55, no. 12, pp. 945–958, 2008.

[13] M. H. Zaman, H. Togashi, and R. E. Baddour, "Deformation of monochromatic water wave trains propagating over a submerged obstacle in the presence of uniform currents," *Ocean Engineering*, vol. 35, no. 8-9, pp. 823–833, 2008.

[14] I. J. Losada, J. L. Lara, R. Guanche, and J. M. Gonzalez-Ondina, "Numerical analysis of wave overtopping of rubble mound breakwaters," *Coastal Engineering*, vol. 55, no. 1, pp. 47–62, 2008.

[15] Y.-G. Cao, C.-B. Jiang, and Y.-C. Bai, "Numerical study on flow structure near two impermeable trapezoid submerged breakwaters on slop bottoms," *Journal of Hydrodynamics*, vol. 22, no. 5, pp. 190–196, 2010.

[16] R. A. Dalrymple, O. Knio, D. T. Cox, M. Gesteira, and S. Zou, "Using a lagrangian particle method for deck overtopping," in *Proceedings of the 4th International Symposium Waves*, pp. 1082–1091, ASCE, September 2001.

[17] H. Gotoh, S. Shao, and T. Memita, "SPH-LES model for numerical investigation of wave interaction with partially immersed breakwater," *Coastal Engineering Journal*, vol. 46, no. 1, pp. 39–63, 2004.

[18] S. Shao, "Incompressible SPH simulation of wave breaking and overtopping with turbulence modelling," *International Journal for Numerical Methods in Fluids*, vol. 50, no. 5, pp. 597–621, 2006.

[19] R. A. Dalrymple and B. D. Rogers, "Numerical modeling of water waves with the SPH method," *Coastal Engineering*, vol. 53, no. 2-3, pp. 141–147, 2006.

[20] S. C. Yim, D. Yuk, A. Panizzo, M. di Risio, and P. L.-F. Liu, "Numerical simulations of wave generation by a vertical plunger using RANS and SPH models," *Journal of Waterway, Port, Coastal and Ocean Engineering*, vol. 134, no. 3, pp. 143–159, 2008.

[21] J. M. Cherfils, L. Blonce, G. Pinon, and E. Rivoalen, "Simulation of water wave—coastal structure interactions by smoothed particle hydrodynamics," in *Proceedings of the 8th International Conference on Hydrodynamics*, Nantes, France, September 2008.

[22] E. Didier and M. G. Neves, "Wave over topping of a typical coastal structure of the portuguese coast using A SPH model," *Journal of Coastal Research*, vol. 56, pp. 496–500, 2009.

[23] S. Shao, "Incompressible SPH flow model for wave interactions with porous media," *Coastal Engineering*, vol. 57, no. 3, pp. 304–316, 2010.

[24] C. Liu, J. Zhang, and Y. Sun, "The optimization of SPH method and its application in simulation of water wave," in *Proceedings of the IEEE 7th International Conference on Natural Computation (ICNC '11)*, pp. 2327–2331, July 2011.

[25] P. W. Cleary, M. Prakash, J. Ha, N. Stokes, and C. Scott, "Smooth particle hydrodynamics: status and future potential," *Progress in Computational Fluid Dynamics*, vol. 7, no. 2-4, pp. 70–90, 2007.

[26] M. B. Liu and G. R. Liu, "Smoothed particle hydrodynamics (SPH): an overview and recent developments," *Archives of Computational Methods in Engineering*, vol. 17, no. 1, pp. 25–76, 2010.

[27] G. R. Liu and M. B. Liu, *Smoothed Particle Hydrodynamics—A Meshfree Particle Methods* , World Scientific Publishing, 2007.

[28] J. J. Monaghan and J. C. Lattanzio, "A refined particle method for astrophysical problems," *Astronomy and Astrophysics*, vol. 149, pp. 135–143, 1985.

[29] J. J. Monaghan, "Smoothed particle hydrodynamics," *Annual Review of Astronomy and Astrophysics*, vol. 30, no. 1, pp. 543–574, 1992.

[30] A. Colagrossi and M. Landrini, "Numerical simulation of interfacial flows by smoothed particle hydrodynamics," *Journal of Computational Physics*, vol. 191, no. 2, pp. 448–475, 2003.

[31] A. Crespo, *Application of smoothed particle hydrodynamics model SPHysics to free surface hydrodynamics [Doctoral thesis]*, 2008.

[32] S. Maiti and D. Sen, "Computation of solitary waves during propagation and runup on a slope," *Ocean Engineering*, vol. 26, no. 11, pp. 1063–1083, 1999.

[33] S. T. Grilli, M. A. Losada, and F. Martin, "Characteristics of solitary wave breaking induced by breakwaters," *Journal of Waterway, Port, Coastal & Ocean Engineering*, vol. 120, no. 1, pp. 74–92, 1994.